DENTAL MATERIALS 35 (2019) 574–584

Available online at www.sciencedirect.com

ScienceDirect

journal homepage: www.intl.elsevierhealth.com/journals/dema

Thermal induced deflection of a porcelain–zirconia bilayer: Influence of cooling rate

M.V. Swain[a,b,*], V. Mercurio[c], J.E. Tibballs[d], M. Tholey[e]

[a] AMME, Sydney University, Australia
[b] Engineering Biomechanics, Don State Technical University, Rostov on Don, Russia
[c] Corob SPA, San Felice s/P, MO, Italy
[d] NIOM a.s., Oslo, Norway
[e] Vita Zahnfabrik GmbH, Bad Sachingen, Germany

ARTICLE INFO

Article history:
Received 28 June 2018
Received in revised form
5 January 2019
Accepted 18 January 2019

Keywords:
Porcelain
Zirconia
Bilayer
Thermal expansion
Cooling rate
Structural relaxation
Fictive temperature

ABSTRACT

Objective. To determine the thermal expansion of a porcelain (VM9) and tetragonal zirconia (Y-TZP) as well as the deflection upon re-heating and cooling of a bilayer fabricated from these two materials after slow and rapid cooling during initial fabrication.

Methods. The coefficient of thermal expansion (CTE) of bulk porcelain and Y-TZP as well as bilayer beam deflection was measured with a novel non-contact optical dilatometer. The influence of cooling rate during initial fabrication of the porcelain–zirconia bilayer and the bulk porcelain during subsequent heating and cooling is investigated. Specimens were heated to 900 °C in the dilatometer, well in excess of the glass transition temperature (T_g) and softening temperature (T_s) of the porcelain.

Results. The thermal expansion of the porcelain above T_g exhibits a threefold increase in CTE over that observed below T_g. Observations of the bilayer deflection reflect the difference in the CTE of the component materials and enable T_g and T_s temperatures for the porcelain to be estimated. Initial cooling rate of the porcelain and porcelain-YTZP bilayer was found to have a profound influence on the subsequent response to slow reheating and cooling as well as the resultant residual deflection.

Significance. The estimation of the residual stress and potential for chipping of porcelain–zirconia dental restorative systems should not be based solely on thermal expansion data measured below T_g.

1. Introduction

Zirconia (primarily yttria tetragonal zirconia polycrystalline Y-TZP ceramics) with its excellent mechanical, biocompatible and aesthetic properties has become of a major dental prosthetic material. In particular, with the CAD/CAM technology having an increasing significant role in the clinic, the use of zirconia for a range of crown and bridge structures is becoming more common [1]. However, the strong optical whiteness, and relatively high opacity, of most zirconia materials has resulted in the veneering of the zirconia with tailored porcelains. Apart from providing the correct shade, the veneering porcelain also improves the aesthetics, enables appropriate

* *Corresponding author at*: AMME, Sydney University, Australia.
E-mail address: michael.swain@sydney.edu.au (M.V. Swain).
https://doi.org/10.1016/j.dental.2019.01.019

translucency, but does require that the thermal expansion properties of the porcelain and zirconia are compatible.

During the past decade, since the introduction of zirconia dental restorations, a high incidence of chipping of the veneering porcelain has been reported [2–7]. The incidence of such chipping observed in these studies has varied from almost non-existent to more than 30% and has raised sufficient concern among the dental community to result in a decline in demand, and to the development of translucent zirconia materials that are used in monolithic form or with a very thin veneering glaze.

Various explanations have been proposed for the origin of the chipping of the veneered structures, amongst others, the development of substantial residual stresses during the fast cooling widely practised in the dental laboratories that fabricate these materials [8]. There have been a number of approaches to investigating the residual stresses present in veneered zirconia structures [9–13]. Isgro et al. [14,15] raised concerns regarding the consequences that thermal expansion mismatch and multiple firing procedures have on the resultant deflection of layered dental structures. More recently Jakubowicz-Kohen et al. [16] investigated the influence of multiple and prolonged firing on the resultant curvature of porcelain zirconia bilayer disks. The extent of the resultant curvature increased with firing time at 900 °C and was suggested as being associated with transformation of the zirconia at the interface [16].

Over the last few years there have been numerous modelling studies [8,17–24] both analytical and numerical (FEA) that have attempted to address the chipping and associated residual stress problem of porcelain veneered Y-TZP. These studies make major assumptions that have limited the ability of these investigations to fully simulate fabrication in the dental clinic or laboratory. In particular, these include knowledge of the glass transition temperature T_g, the visco-elastic softening temperature T_s, the thermal expansion coefficient above T_g and the temperature dependence of the elastic properties of the specific porcelains simulated. Regulatory approval has only required that the thermal expansion coefficient values for porcelains be quoted for temperatures below T_g. These have been measured on large-diameter rods, which are generally not fabricated in the same manner as the dental restorations. Another factor that has been barely explored is the role of structural relaxation or density development of the porcelain from its liquid state to glassy state on cooling [25]. Together these assumptions impart considerable uncertainty on the relevance of the modelling studies undertaken.

Veneering porcelains tend to be predominantly glassy with no defined melting temperatures and with features that are typical of glasses, namely that the glass transition temperature, T_g, and room-temperature density of the glass depend on cooling rate [25]. The CTE below T_g is generally considered almost completely independent of cooling rate however various relaxation effects may occur during reheating. Another factor for veneering porcelains is the development of increasing content of leucite with slower cooling rate and longer hold time above 500 °C [26–28].

Bilayer materials have long been used for thermostat control and were the basis of a classic thermo-elastic mechanics analysis by Timoshenko 90 years ago [29]. Some 30 years ago there were investigations of the deflection response of metal-porcelain bilayer systems by Lenz et al. [30]. More recently Kvam and Hero [31] used bilayer deflection to investigate the relaxation and residual stresses in titanium-porcelain bilayers. In another study Twiggs et al. [32] used bilayer porcelain fused to metal (Ni–Cr alloy) to investigate the influence of changes in leucite content by isothermal heat treatment on the resultant bilayer deflection to determine the low temperature (≤300° C) CTE. Asaoka et al. [33–35] also investigated the role of visco-elastic deformation of porcelain on the residual stresses developed during fabrication of porcelain fused to metal structures including bi- and tri-layers. They were able to include the role of cooling rate on the resultant deflection and the resultant residual stresses developed. This was achieved by using incremental time steps during cooling that allowed the temperature of slices through the veneer/metal slab to be determined along with the glass transition temperature, effective E modulus, creep strain, thermal expansion which enabled the internal stresses and resultant beam curvature to be calculated [35]. Another key contributor to this area is the seminal work of Scherer [36] who almost 30 years ago published his classic monograph on relaxation in glass and composites. In this book Scherer considers the critical roles of cooling rates on the resultant properties of glass, be they density, refractive index or electrical conductivity. Another key aspect is the concept of fictive temperature T_f introduced by Tool [37] to rationalise structural relaxation or densification of glass and which was critical for generating a complete understanding of glass tempering by Narayanaswamy [38,39].

In this paper a simple porcelain–zirconia system is investigated to determine the relevant thermal expansion coefficients of both materials and critical T_g and T_s temperatures of the porcelain. The effect of two initial cooling procedures on the resultant porcelain expansion and bilayer deflection is also considered.

2. Materials and methods

2.1. *Specimen preparation*

In this study yttria-stabilized, tetragonal zirconia polycrystalline ceramic (Y-TZP, VITA In-Ceram® YZ, VITA Zahnfabrik, Germany) was used as the elastic substrate material. The specimens were prepared by sintering at a temperature of 1530 °C for 2 h. For the observation of the bilayer deflection experiments, rectangular plates (sample bars) with dimensions of 44 × 4 × 0.5 mm were used, the specimens for the CTE were approximately 15 × 5 × 5 mm. As veneering porcelain, the natural-feldspar-based VITA VM® 9 (VITA Zahnfabrik, Germany), was built up on the zirconia surface using the methods listed in Tholey et al. [9]. The porcelain CTE specimens had the same dimensions as the zirconia.

For both preparation methods a dentine firing, an enamel firing and a glaze firing were applied to simulate a typical work process to create a porcelain veneer with a total thickness of 0.8 mm. Details of the firing of the porcelain veneer on to the Y-TZP are given in Tholey et al. [9]. The final cooling procedures were as follows: the slowly cooled specimen remained in the firing furnace Programat P95 (Ivoclar Vivadent, Liechtenstein)

to 500 °C before removal, while the rapidly cooled specimen was removed from the furnace at the end of the hold period at the maximum temperature and placed on a ceramic thermal shock resistant plate resting on the enamelled aluminium base of the furnace.

2.2. Thermal expansion and bilayer deflection

Two non-contact optical dilatometer systems were used. For determination of the intrinsic thermal expansion of the porcelain and zirconia materials a vertical optical dilatometer was used (Misra® ODLT, Expert Systems Solutions, Modena Italy). This system has two optical paths and utilizes microscopes with high magnification, with which both ends of the sample are framed. The first optical path measures the position of the top of the specimen while the second optical path is focused on the sample holder thereby providing a reference beam. The specimens were heated at 10 °C/min to 660 °C.

After the thermal expansion measurement of the porcelain the temperature was cycled three times between 660 °C and 450 °C with cooling rates of 2 °C/min and heating rates of 5 °C/min before final cooling as shown in the insert in Fig. 3.

To investigate the porcelain–zirconia bilayer elastic and viscous deformation an optical fleximeter was used [Misura® Flex, Expert Systems Solutions, Modena Italy]. The sample bar is suspended on two supporting rods spaced 25 mm apart, while a camera is focussed on the centre of the sample. This moves both downward or upward as the bar bends and unbends during heating or cooling. In each instrument, a split beam of blue light, enables movements to be measured at a resolution of 0.5 μm. The bilayer mid-point displacement–temperature relationship obtained upon heating allows the identification of the thermo-elastic coupling between the porcelain and zirconia associated with the thermal expansion mismatch until viscous relaxation occurs upon exceeding the porcelain softening temperature, T_s, at which temperature the beam straightened. The temperature-dependence of the displacement of the bilayer mid-point was obtained by heating from room temperature at 30 °C per minute, recording displacements at 1 s intervals until the displacement began to decrease. Because the CTE of the porcelain changes at T_g, there is also a change in slope of the bilayer temperature–displacement curve. On cooling the development of a state of residual stress is deduced from the residual flexure of the bilayer. Two repeats of each measurement test were made and found to be reproducible within ±5 μm.

2.3. X-ray diffraction (XRD)

X-ray diffraction scans were conducted on planar disks of rapidly and slowly cooled VM9 to estimate the leucite content. Scans between 20 and 40° theta were made with 0.01° steps and 12 s counting per step, using Cu K_α radiation.

2.4. Theoretical bilayer deformation

The coupling between components of the bilayer, in this case porcelain and zirconia, was evaluated based on Timoshenko [29] for the curvature induced in a homogeneous, isotropic elastic bilayer by thermal expansion mismatch. The analysis has some simplifying assumptions: namely, a perfect interface with no structural changes, uniform temperature through the bilayer during cooling and a constant ratio of elastic moduli during heating and cooling. The deflection, D, of the mid-point for the bilayer shown in Fig. 1 is given by:

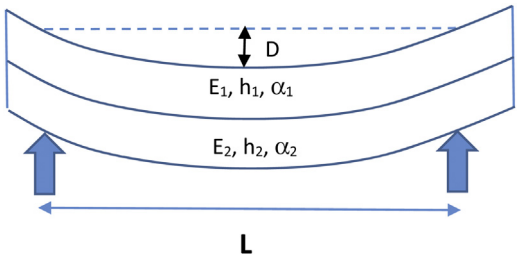

Fig. 1 – Schematic simplified model of the bilayer deflection.

$$D = \frac{L^2 \kappa}{8} \tag{1}$$

where L is the span between the supports, h is the thickness of the bar and the inverse radius of curvature κ of a bi-material beam is given by,

$$\kappa = \frac{6E_1E_2(h_1+h_2)h_1h_2\varepsilon}{E_1^2h_1^4 + 4E_1E_2h_1^3h_2 + 6E_1E_2h_1^2h_2^2 + 4E_1E_2h_2^3h_1 + E_2^2h_2^4} \tag{2}$$

where E_1 and h_1 are the Young's modulus and height of the veneer and E_2 and h_2 are the Young's modulus and height of the substrate. The term ε is the thermal expansion misfit strain, calculated by:

$$\epsilon = (\alpha_1 - \alpha_2)\,\Delta T \tag{3}$$

where α_1 is the coefficient of thermal expansion of Material One and α_2 is the coefficient of thermal expansion of the substrate. ΔT is difference between the current temperature and the reference temperature at which the beam exhibited no flexure.

2.5. Finite element analysis of thermal transients

Rapid bench cooling in which a specimen with a flat face is placed on a room temperature bench plate leads to a much higher heat loss through the contact face than by radiation and convection through the other surfaces. By matching transient temperatures evaluated using finite-element software Lisa [version 8.0.0, Sonnenhof Holdings, Mississauga, OT, Canada] to temperatures measured in previous studies [9,10], which followed similar cooling procedures with veneered platelets and thermocouples embedded at the veneer surface and at the veneer-substrate interface, appropriate thermal conductivity and heat capacity properties could be assigned to a 50 μm thick layer assumed to separate the specimen and the bench plate. With these same boundary conditions, cooling curves were obtained for the thermal expansion specimens and bilayer specimens employed in the present study. The calculations included radiative and convective heat loss via surfaces exposed to air at ambient temperature and included

Table 1 – Thermal expansion of the Y-TZP and fast and slow cooled porcelain blocks.

Material Property	Y-TZP	Slow cooled porcelain	Fast cooled porcelain
T_g		560 °C	580 °C
CTE below T_g	10.5 ppm/K	9.3 ppm/K	Heating 7 ppm/K Cooling 9.4 ppm/K
CTE above T_g	10.5 ppm/K	24.6 ppm/K	Heating 51 ppm/K Cooling 36 ppm/K

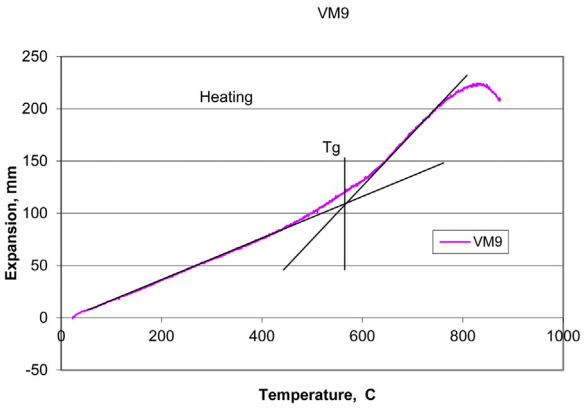

Fig. 2 – Thermal expansion of the slowly cooled porcelain (VM9) upon heating to 920 °C as measured with the optical dilatometer. CTE and T_g in Table 1 are estimated by fitting the lines as shown. The deviation from linear behavior at approximately 750 °C marks the onset of flow of the porcelain under its own weight. The maximum elongation corresponds to a viscosity of approximately 10^8 Pa s.

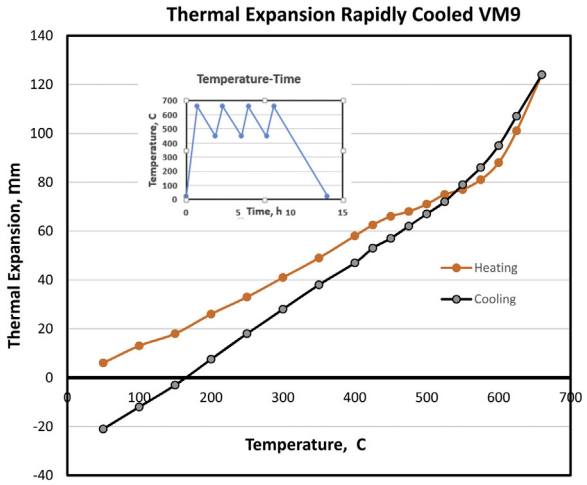

Fig. 3 – Thermal expansion of the initially rapidly cooled porcelain specimen during heating to 660 °C and final cooling from 660 °C. The temperature-time multiple thermal cycling between 450° and 660 °C prior to final cooling is indicated in the insert. Note the significant differences in the slope of the initial heating and final cooling curves as well as the change of slope between 450° and 575 °C on the initial heating curve.

a ten-second period of convective air cooling for the transfer from the furnace to the bench.

3. Results

3.1. *Thermal expansion of porcelain and zirconia*

The thermal expansion of the slowly cooled porcelain, is shown in Fig. 2. The porcelain exhibits four distinct regimes; linear expansion below 450 °C; a slight increase in expansion coefficient to 600 °C; a considerable increase to 720 °C; above this temperature, viscous relaxation under the own weight of the upright bar that leads to maximum elongation at ~820 °C. The standard linear coefficients of thermal expansion of the porcelain and zirconia and T_g for the porcelain derived from these data are given in Table 1.

The initial thermal expansion and final contraction curves of the porcelain specimen that was initially cooled rapidly are shown in Fig. 3. There is a substantial difference between the slopes of the initial heating and final cooling curves with the sample contracting by an additional ~25 μm during final cooling. The rapid initial heating rate of 10 °C/min may have resulted in a small temperature gradient through the block but this is not expected to be the major cause of the substantial dimensional hysteresis observed. This is a dimension reduction of 0.16% which corresponds to a density increase of 0.48% for the porcelain. Notice there is also a significant reduction in the slope of the initial re-heating curve between 450 °C and 575 °C before the slope increases. The T_g on the heating curve appears to be at ~580 °C whereas on the cooling curve it is ~560 °C. The CTE of the initially rapidly cooled porcelain on heating and final cooling between 50 and 450 °C are listed in Table 1.

3.2. *Porcelain/Y-TZP bilayer*

The deflection response of the initially slowly cooled porcelain–zirconia bilayer upon heating at 2 °C/min to 900 °C and cooling at the same rate is shown in Fig. 4(a). The gradient of the deflection versus temperature upon heating is initially negative until a temperature of ~500 °C whereupon it changes to a steep positive gradient to 650 °C when it again reverses before coming to a plateau at ~700 °C with a deflection of +30 μm. On cooling there is slight positive gradient that commences at ~700 °C, which increases significantly between ~650 and 550 °C before becoming negative and following a similar curve to that observed during heating.

For the initially rapidly cooled bilayer specimen the response to heating and cooling to 900 °C at 2 °C/min is shown in Fig. 4(b). The gradient of the deflection versus temperature is steeply negative to 400 °C becomes even steeper to ~580 °C (T_g upon heating). Above 580 °C the slope becomes very steep and positive till the temperature reaches ~650 °C where it

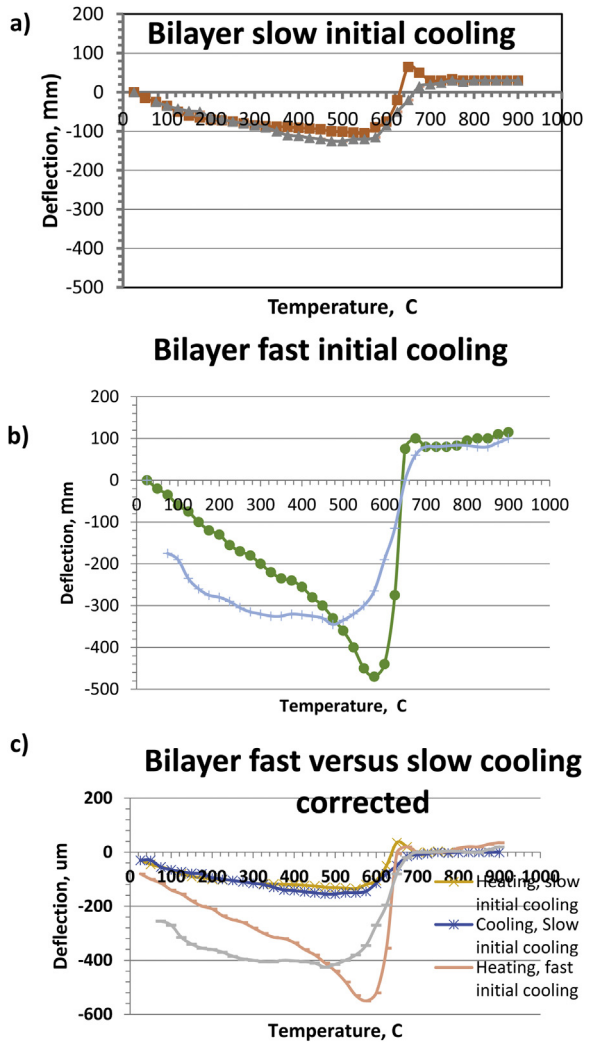

Fig. 4 – (a) Bilayer deflection upon heating and cooling to 900 °C for the initially slow cooled specimen. (b) Bilayer deflection for the initially rapidly cooled specimen. (c) Corrected deflections for (a) and (b) based upon the assumption that the zirconia substrate is under no stress from the porcelain at temperatures above 700 °C (>T_s) and as such there is zero deflection of the bilayer.

changes slope and becomes negative again before plateauing at ~700 °C with a deflection of +80 μm. Upon cooling the gradient becomes positive below 700 °C then it rapidly increases before going through a turning point at ~480 °C (T_g upon cooling) with a negative gradient that persists till below 100 °C but with a far less steep slope than the initial heating curve. If the cooling curve is extrapolated back to room temperature, which was not done because of the time to cool at such low temperature differences from ambient, then a negative offset deflection of ~125 μm is estimated.

If one makes the assumption (as did Twiggs et al. [32]) that the plateau regions in Fig. 4(a and b) above 700 °C, are regions where the viscosity of the porcelain has become so low that is it has reached the softening temperature T_s for the rates of heating used, consequently no longer are differences in CTE able to cause deflection of the zirconia elastic beam. That is these plateau deflections of the bilayer are indicative of zero defection of the elastic zirconia substrate and so may be used as the basis to superimpose the curves shown in Fig. 4(a and b) enabling the residual deflection of the bilayer beams at room temperature as shown in the corrected bilayer deflection, Fig. 4(c). The plots in the latter curves suggest that the bilayer was deflected upon initial cooling with the fast initial cooled bilayer having a much greater deflection (−80 μm) than the more slowly cooled sample (−30 μm). This figure also suggests that for the initially rapidly cooled bilayer upon reheating and slowly cooling the residual deflection is much greater (≃150 μm).

The coupling temperature or the set temperature (see Scherer [36]) at which the onset of stress develops upon cooling is expected to be cooling-rate dependent and for the 2 °C/min cooling curves this occurs at ~700 °C but is more evident at 660 °C when the slope of the curves increases. The observations shown in Fig. 4(c) are almost identical to that proposed by Asaoka [35] for the slowly cooled bilayer as there is no difference between the reheating and cooling response.

3.3. *XRD Results*

The powder diffraction intensity (Fig. 5(a)) shows the small leucite 400 and 420 peaks at $2\theta = 27.25$ and 30.5°, respectively with evidence of several other crystalline components, on the broad amorphous background. The differences between rapidly and slowly cooled specimens in the 2θ ranges about these peaks are shown in Fig. 5(b and c). The fraction of crystalline leucite in the rapidly cooled specimen, as estimated from peak area intensities, was less than 4% with less than an extra 2% leucite in the slowly cooled specimen. This approach, as shown by Ong et al. [40], results in a higher estimate of the volume fraction of leucite than from estimates derived from peak height ratios.

3.4. *Bilayer deflection simulation*

Simulation of the bilayer deflection for initial heating based upon the Timoshenko expression, as presented in Eqs. (1)–(3), was undertaken. The results are shown in Fig. 6 for the slowly and rapidly cooled specimens and may be compared with the results in Fig. 4(a and b). No attempt was made to simulate the cooling curves as, although these match the slowly cooled sample, the difference in the case of the rapidly cooled specimen are significant. The slowly cooled sample could be matched with just the two values of the CTE for the porcelain, below and above T_g. The simulation was made using the values of E_1 (porcelain) of 69 GPa, E_2 (Y-TZP) 210 GPa, thickness of porcelain 0.8 mm and Y-TZP of 0.5 mm, the thermal expansion of the Y-TZP material (10.5 ppm/K). For the slowly cooled sample the required mismatch was −2 ppm/K implying the CTE of the porcelain below T_g was 8.5 ppm/K. For the region of the curve above T_g and below T_s the required mismatch was +17.5 ppm/K implying a CTE of the porcelain of 28 ppm/K. For the rapidly cooled sample, the much stronger deflection response to temperature change required the use of two values of the CTE mismatch below T_g. From 20 to 400 °C the mismatch was assigned −7 ppm/K and between 400 and 550 °C

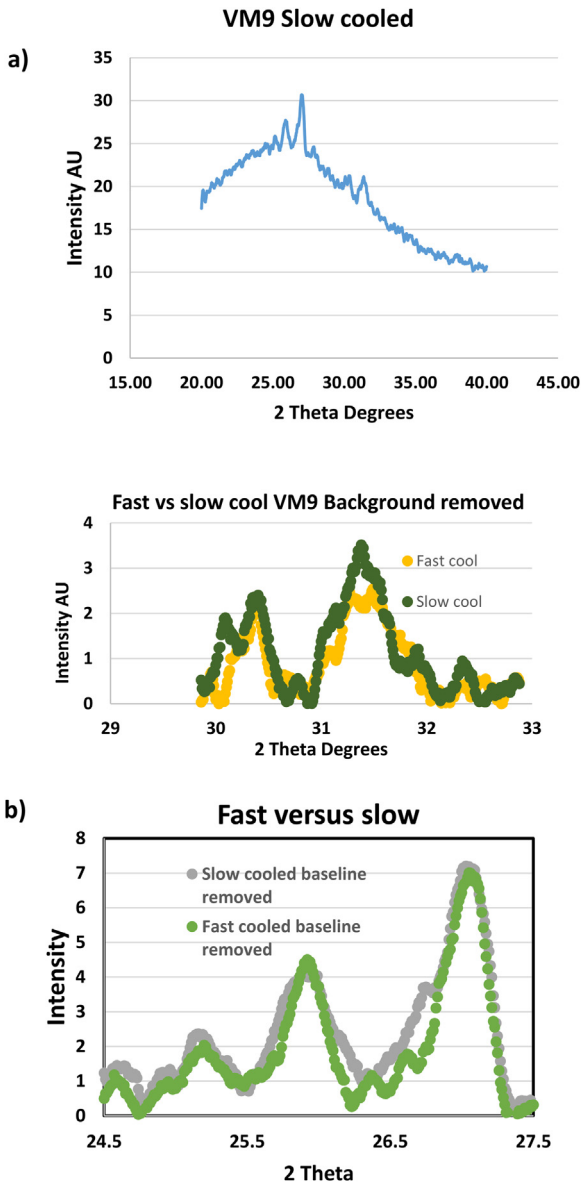

Fig. 5 – (a) XRD results for the slow cooled diffraction pattern of VM9. (b) Comparison of the leucite peaks following fast and slow cooling after removal of the broad amorphous background.

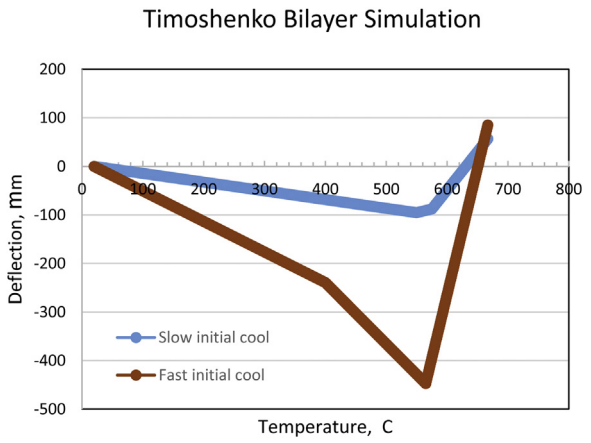

Fig. 6 – Simulated porcelain-YTZP bilayer deflection upon reheating of the fast and slow initially cooled specimen based upon Eqs. (1)–(3). The values assumed for CTE to match the experimental observations are listed in the text.

−14 ppm/K. These imply that the effective CTE of the porcelain over these temperature ranges was 4.5 ppm/K and −3.5 ppm/K respectively. At temperatures between T_g and T_s, i.e. between 580 and 650 °C, the mismatch required was +58 ppm/K or an effective CTE for the porcelain of 42.5 ppm/K.

3.5. *Finite element analysis of thermal transients*

The temperature gradients and transients induced by bench cooling of fired specimens evaluated by finite-element analyses of three specimen configurations: (i) the 5 × 5 × 15 mm thermal expansion specimens, (ii) the 1.3 × 4 × 44 mm beam-deflection specimens and, for reference, (iii) the 3 × 5 × 15 mm veneered specimens of Choi et al. [10]. The important difference is in the cooling rate at which the specimens pass through the temperature range of the glass transition temperature. Defining this range as 650 °C to 550 °C, the rates are calculated as shown in Table 2. In addition, the temperature gradients across the porcelain and the substrate have been evaluated as appropriate. For comparison, the cooling rate for slowly cooled specimens was 1 K s^{-1} with temperature differences less than 1 K.

Table 2 Cooling rates and temperature gradients of bench-cooled specimens as evaluated by finite-element analysis for thermal-expansion, beam-deflection and reference specimens.

4. Discussion

The thermal expansion of the Y-TZP material is linear up to 900 °C, with the CTE value agreeing with that provided by the manufacturer and with values in the literature [41]. Over the range 20–450 °C, the thermal expansion of the VM9 is close to linear and again the CTE matches that stated by the manufacturer, namely 9.1 ppm/K. Above 450 °C the observed elongation with temperature depends on the previous rate of cooling. The length attains a maximum at 820 °C the temperature at which the viscous flow of the porcelain cylinder under its own weight is balanced by the thermal elongation. This effect is associated with a viscosity of ~10^8 Pa s [25].

It is helpful to consider the conceptual issues to give a physical perspective as a bilayer visco-elastic/elastic system is cooled and then reheated.

Consider initially the specific volume of the porcelain in a bilayer that is free of temperature gradients as it is rapidly or slowly cooled then slowly reheated. The outcomes are as shown schematically in Fig. 7(a), with the change in specific volume change for Y-TZP shown for comparison, with the two volumes set to be equal at the temperature, T_{couple}, at which the porcelain becomes stiff enough to couple to a substrate. Immediately before the temperature attains T_g on reheating a rapidly cooled porcelain, the density increases due to

Table 2 – Cooling rates and temperature gradients of bench-cooled specimens as evaluated by finite-element analysis for thermal-expansion, beam-deflection and reference specimens.

Specimen	5 × 5 x 15 mm CTE	1.3 × 4 x 44 mm veneer/substrate	3 × 5 x 15 mm Choi
Cooling rate [K s^{-1}] 650 °C–550 °C	12	50	24
Temperature difference [K]	157	40/6	28/37
Temperature gradient [K mm^{-1}]	31	50/12	19/25

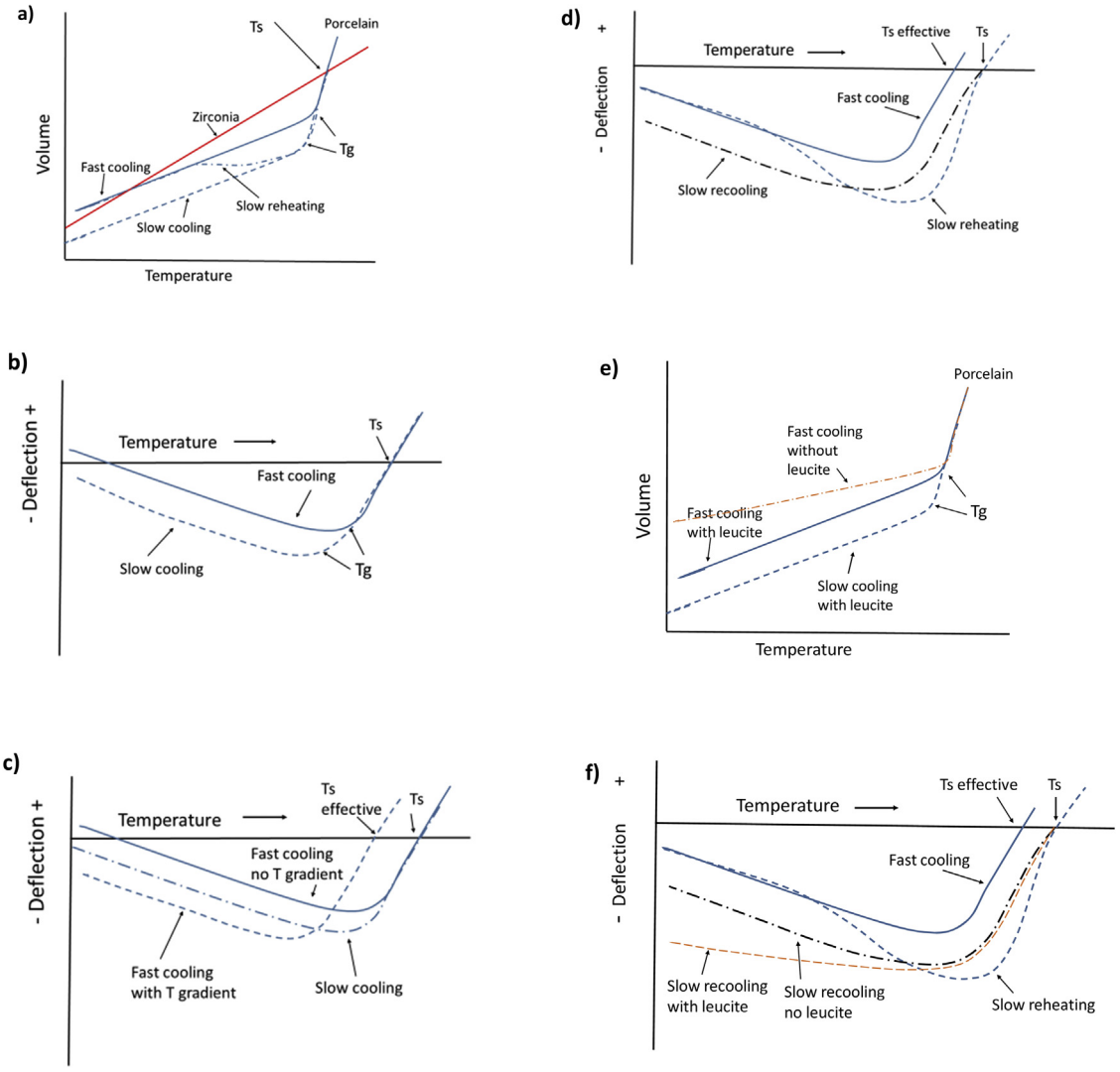

Fig. 7 – Schematic representations of; (a) the volume change of fast and slow cooled porcelain compared with YTZP. (b) Porcelain-YTZP bilayer deflection assuming that the T_s temperature is independent of cooling rate. (c) Bilayer deflection assuming the effective T_s temperature is reduced, especially at the porcelain–zirconia interface, because of the temperature gradient developed through the bilayer during fast cooling. (d) Bilayer deflection for the rapidly cooled sample upon slow reheating and re-cooling. (e) Porcelain rapid versus slow cooling with and without the presence of leucite. Notice that the absence of leucite decreases the CTE below T_g. (f) Bilayer deflection incorporating the concept of fast initial cooling effectively reducing the T_s temperature and upon reheating reducing the CTE but having major structural densification, which upon recooling with normal T_s, and the formation of leucite results in a higher CTE of the porcelain and less recovery of the deflection of the bilayer.

structural relaxation, towards the density of the slowly cooled porcelain. Fig. 7(a) matches the experimental results in Fig. 3 and also the expectation from glass relaxation processes [33]. The T_g observed for rapidly cooled porcelain will be slightly higher than for slowly cooled porcelain while the CTE well below T_g is independent of cooling rate.

If we now consider a bilayer situation, for the normal case in which the CTE of the porcelain is less than the substrate material, resulting in a slight upward deflection of the cooled specimen, then porcelain is in compression at room or body temperature. For the rapidly cooled sample, the porcelain is in tension at the interface, since the change in specific volume of

the porcelain on cooling has now become less than the zirconia. This assumes a constant coupling temperature, T_{couple} at which the porcelain becomes stiff enough, to exert stress on zirconia. The outcome for the deflection response of a bilayer upon cooling, assuming no temperature gradients, is shown in Fig. 7(b). However, Tholey et al. and Choi et al. [9,10] have measured up to 100 °C temperature difference between the surface and interface temperatures of bilayers at comparable cooling rates. If we acknowledge a large temperature difference between the surfaces of the ceramics and their interface and that it is only when the interface reaches T_{couple} that the bilayers become coupled, then the result is as shown schematically in Fig. 7(c). That is, the apparent T_{couple} is substantially lowered and the experimental curve for the rapidly cooled specimen, based on an external temperature measurement, is moved to lower temperatures causing a greater upward residual deflection of the bilayer upon cooling. This cooling rate response is precisely what the porcelain fused to metal bilayer analysis of Asaoka [35] predicts. Upon reheating, the slowly cooled bilayer follows a very similar deflection response to that seen during the initial cooling.

Upon reheating, the rapidly cooled sample initially follows the cooling response, but, prior to attaining T_g, structural relaxation allows the glass to densify. During densification, the volume decreases at a rate dependent upon the rate of heating until T_g has been reached. Above T_g and below T_{couple} the fluid-like expansion of the porcelain determines the CTE of the glass is much greater than Y-TZP resulting in a change of deflection rate as illustrated in Fig. 7(d). Upon slow re-cooling of this slowly reheated porcelain, the initial rapid deflection below T_{couple} will change at T_g to a curve almost parallel to the slowly cooled sample but, because the specific volume has decreased (density increased), the resultant residual deflection upon cooling is much greater than both the slowly cooled and rapidly cooled specimens as also shown in Fig. 7(d). The latter behaviour is closely matched by the experimental reheating and re-cooling results for the bilayer in the "corrected" curve shown in Fig. 4(c).

As shown in Fig. 3, the thermal expansion of the rapidly cooled porcelain differs substantially between reheating and subsequent cooling. The response upon final cooling is very similar to that initially measured for the slowly cooled specimen. Up to 400 °C, a linear expansion with a value of 7 ppm/K while between 400 and 550 °C, the apparent coefficient of expansion is much lower at 5.3 ppm/K. This reduction in CTE below T_g is associated with structural relaxation occurring within the glass because at the slow heating rate there is sufficient time to allow partial densification to occur [36]. The dimensional contraction of the sample, ~25 μm or 0.16%, which, if assumed similar in the orthogonal directions, implies 0.48% (3*Δl) increase in the density of the porcelain. The increase in density is most noticeable upon reheating between 400 and 550 °C, the T_g of the porcelain. As discussed and illustrated by Scherer [36] (see Fig. 9.11 of his monograph on soda-lime glass data from Ritland [42]), the density of glass is a function of the cooling rate. Typically, on a change in cooling rate from 100 to 0.1 °C/h there is a density increase of ~0.45%. In the present case the cooling rate varied from approximately 30–0.03 °C/s for the rapid and slowly cooled sample; i.e. similar range to that employed by Ritland presumably with comparable change in density [42]. According to Narayanaswamy [39] the change in density of a glass is given by

$$\Delta\rho/\rho_0 = 3a_s\Delta T_f$$

where a_s is the structural expansivity of "liquid" glass ($\alpha_s = \alpha_l - \alpha_g$)(~(24.6–9.2) ppm/K) and ΔT_f is the difference in the *fictive* temperature T_f between rapid cooling and subsequent slow cooling. The present results based upon the above expression suggest that the change in fictive temperature is approximately 100 °K. This value of ΔT_f is very large, and the greatest reduction in density would be expected at the external surfaces of the porcelain as it is here the fictive temperature gradient is greatest [39]. Observations of multiple cycling between 450 and 660 °C (Fig. 3) showed minimal further change in the expansion response. Another possible contribution to the increase in the rate of thermal expansion during re-cooling comes from the increase in the volume fraction of leucite [26–28]. This issue will be discussed below.

The much lower thermal expansion upon slow reheating to 400 °C of the rapidly cooled porcelain is surprising but reproducible. A possible interpretation is that there are significant thermal gradients during initial cooling, especially in the range T_{couple} to T_g. Such gradients cause the tempering stresses that develop in glassy and visco-elastic materials. This feature is clearly illustrated in Kingery et al. [25] based on observations in glass plates by Gardon and Narayanaswamy [43]. More detailed calculations of the residual stress in glass by Narayanaswamy [39] show that structural relaxation plays a key role in the determination of the residual stresses and is able to predict the resultant density gradients within tempered glass. If one considers the temperature gradients present during rapid cooling then these are typically 100 °C between the surface and the centre of the specimen. However, the bulk of the material is always much hotter than the surface because of the low thermal conductivity of glassy (porcelain) materials. In the temperature range below 400 °C, on initial cooling the surface temperature may be 100 °C below the interior when the latter is at T_g. So while the interior cools to ambient from T_g developing the tempering tensile stresses, the surfaces have already cooled (T_g-100). That is, the effective contraction possible is related to $\{(T_g - 100)/T_g\}^*\alpha$, or for the present case where T_g is ~560 °C, α_g is 9.3 ppm/K the effective CTE is 7.3 ppm/K, which is closer to what was measured.

The thermal deflection of the porcelain/Y-TZP bilayer (Fig. 4) again showed substantial differences between rapidly and slowly cooled specimens. The slowly cooled bilayer (Fig. 4(a)) showed a reversible response with clearly defined slopes below and above the T_g as well as minimal further deflection above T_{couple}. The rapidly cooled bilayer (Fig. 4(b)) showed much greater deflection upon reheating with far greater temperature dependence both below and above the T_g of the porcelain. Again at T_{couple} there is minimal further deflection. If the data are "corrected' by assigning the T_{couple} temperature to the temperatures at which the deflections of cooled samples show minimal further change, then these two bilayer conditions can be compared as shown in Fig. 4(c). Considering first the slowly cooled bilayer, there is a small residual deflection of ≃30 μm upon cooling to RT indicative of a compressive strain within the porcelain. An estimate of the

surface residual compressive stress based upon the measured deflection, resultant radius of the bilayer and its equivalent (of either component, see Ref. [44]) thickness is a compressive strain of 0.44×10^{-3} (porcelain) and 0.167×10^{-3} (zirconia) at the interface and with the known E of the porcelain (69 GPa) the stress is 30 MPa and for the zirconia (E = 210 GPa [41]) it is 35 MPa. For the rapidly cooled bilayer, the initial deflection is much larger as shown in the corrected curve in Fig. 4(c) and is ≃80 μm. Based upon the same analysis the magnitude of the surface compressive stress in the porcelain is 82 MPa and for the zirconia a tensile stress of 93 MPa. These values of porcelain residual compressive stress are similar to values measured by Choi et al. for porcelain–zirconia bilayers subjected to different cooling rates [10]. The situation upon subsequent slow re-cooling of the rapidly cooled sample indicates that the residual deflection of the bilayer has greatly increased because the T_{couple} temperature is now unaffected by temperature gradient though the bilayer and greater structural relaxation (densification) can occur during cooling. The resultant deflection is now almost 3 times the value seen for the rapidly cooled specimen. This suggests a compressive stress of >100 MPa. An interesting feature of the present result is that even with reheating of the bilayer sample to 900 °C, well above the T_{couple} temperature, there is much more substantial deflection than the initial slow cooled bilayer.

Another feature of the results for the rapidly cooled bilayer is that CTE found on reheating of rapidly cooled porcelain up to 400 °C is very low, 4.5 ppm/K, which is not related to structural relaxation effects. Following the argument made above for the effective CTE of the rapidly cooled bulk porcelain, a similar situation would arise for the porcelain in the bilayer. In fact, in the bilayer the situation would be emphasised because there is a greater thermal gradient associated with the higher heat transfer possible with a thinner specimen and also even more of the porcelain would be at higher temperatures since one side of the specimen is YTZP which is also a poor thermal conductor. For the bilayer, the present results suggest that the temperature difference is greater than for a uniform porcelain specimen and that a greater volume of glass remains hot thereby contributing to an even lower interface contraction for the porcelain. In addition, the temperature at the porcelain–zirconia interface determines the temperature for the coupling between the materials and this will determine when deflection of the bilayer, because of thermal expansion mismatch, begins. This interpretation is supported by the subsequent slow re-cooling where the slope of the deflection temperature curve as shown in Fig. 4(b and c) is very similar to that of the originally slowly cooled bilayer and having comparable thermal expansion.

An alternative explanation of the results shown in Figs. 3 and 4 (b), both for the fast cooled porcelain cylindrical sample and the fast cooled bilayer, is to consider the behaviour of the porcelain to be related to the nucleation of additional leucite during cooling. If we consider that during initial specimen firing at 900 °C there is limited leucite present in the porcelain and that as shown by Mackert et al. [26–28] a substantial increase (9–56%) develops upon slower cooling with similar cooling protocols as used in the current experiments. As shown by Mackert et al., in a slowly cooled sample there is a considerable volume fraction increase of leucite resulting in a much greater CTE up to 450 °C. For the rapidly cooled samples, however, only a limited volume fraction of leucite is present in the VM9 porcelain. Upon reheating these rapidly cooled samples, the initial CTE would be lower than the slowly cooled samples because there was less leucite present. However, upon re-cooling these samples from 900 °C, at a much slower rate than the initial cooling curves, considerably more leucite may be formed resulting in a much higher CTE. The situation, according to Palmer et al. [45] from neutron powder diffraction data, is that the atomic positions and "thermal" displacements are more complex as there appears to be an order-dependent component. Additional work by Newton et al. [46] consider two ordering parameters, associated with the K atom position, one of which they link to the tetragonal c/a ratio and the other to the volume change. From their analysis one concludes that leucite does not order fully even at low temperature rather it only achieves about 90% order. The role of rapid quenching on such ordering is poorly understood, but it is considered that it may be "frozen-in" with consequences for the resultant expansion of the leucite present.

Taylor and Henderson [47] have determined the lattice dimensions and unit cell volume of leucite crystals using X-ray diffraction observations at temperatures from RT to 1000 °C, which covered the tetragonal to cubic phase transformation at 690 °C. Taking the data from Taylor and Henderson the CTE of leucite is very temperature sensitive and to a good approximation at temperatures below T_g of the porcelain is given by

$$\alpha_L = 0.1513T + 4.5468$$

where T is the temperature in °C. Then using the simple rule of mixtures for the expansion of the glass leucite composite, namely [36]

$$\alpha_p = \alpha_0 (1 - V_L) + \alpha_L V_L$$

where α_p is the CTE of the porcelain, α_0 is the CTE of the glass, V_L is the volume fraction of leucite. We can now estimate the increase in the leucite volume fraction, V_L, upon recooling from the difference in thermal expansion.

We are now in a position to consider the rapidly cooled porcelain specimen and the difference in thermal expansion between initial reheating and subsequent re-cooling as shown in Fig. 3. Assuming that the rapidly cooled sample has a very small amount of leucite present upon reheating then upon subsequent re-cooling an additional 7–8 vol% of leucite is required to increase the averaged thermal expansion (25–450 °C) from 7 to 9 ppm/K as observed. This aspect is shown schematically in Fig. 7(e). However, based upon the XRD results in Fig. 5 the total amount of leucite present in VM9, even after slow cooling, is estimated at less than 6% and far less than that required to cause the changes in thermal expansion observed.

The above suggested change in the leucite content as a function of initial cooling rate does not account for the very low thermal expansion of the porcelain (4.5 ppm/K) over the temperature range 25–400 °C required to match the value deduced from the bilayer deflection upon reheating after rapid cooling. This value is well below that for a glass with the same composition as the porcelain. The reduced "effective" T_{couple}

for the porcelain of the rapidly cooled bilayer and the limited presence of leucite together provide a basis to rationalise the low thermal expansion of the porcelain required upon initial reheating, especially below 400 °C. Upon heating above 400 °C structural relaxation is anticipated and observed along with the possibility for the nucleation of leucite. Both of these may contribute to substantially lower initial expansion of the bilayer porcelain material. Further precipitation of leucite may occur during heating above T_g and would be expected to enhance the effective expansion of the glass as the thermal expansion of leucite becomes very high (80–100 ppm/K) as the temperature approaches the tetragonal-to-cubic phase transformation temperature (660 °C). On subsequent re-cooling from elevated temperature, as in Fig. 4(b), and the higher effective thermal expansion of the porcelain, matching the experimental results below T_g, maybe related to the presence of leucite and the T_{couple} and T_g not being associated with a significant thermal gradient through the bilayer. The latter is depicted schematically in Fig. 7(f).

To enable further understanding of this topic additional information, including the measurement of bilayer deflection during the rapid or slow cooling after firing along with thermocouple measurements from the surfaces and porcelain–zirconia interface are required. Such observations would provide a basis to verify whether the schematic concepts shown in Fig. 7(d) and (e) are realistic. Interpretation of all the results and development of a comprehensive analytical model, which includes prediction of the structural and visco-elastic relaxation of the porcelain plus the presence of leucite on the bilayer deflection and state of residual stress development, requires a follow up of the Scherer analysis along the lines referred to by Kvam et al. [48].

5. Conclusions

Optical dilatometers enable non-contact assessment of the CTE to well above the T_g, and for bilayer structures the T_s temperatures and resultant residual deflections are clearly evident.

Rapidly cooled porcelain (VM9) shows substantially lower CTE on reheating than slow cooled specimens, an effect which is more pronounced for the bilayer. For the bulk and somewhat more slowly cooled sample the change in CTE from approx 7–9 ppm/K upon slowly reheating and re-cooling may be partially related to an increase of leucite associated with slow re-cooling.

Relaxation of stresses during heating and development of stresses during cooling within the bilayer takes place at temperatures well above T_g. The CTE of porcelains above T_g is up to 3 times that below T_g and the must be considered in any modelling analysis of the resultant residual stress state of a bilayer.

Upon slower reheating, rapidly cooled porcelain and bilayer samples exhibit structural relaxation or glass densification below T_g.

Slow reheating and re-cooling of initially slowly cooled Y-TZP–porcelain bilayer closely follows a classic thermo-elastic analysis.

Initially rapidly cooled bilayers exhibit greater residual deflection and upon slow reheating and re-cooling the residual deflection increases. The porcelain CTE required to match the slower reheating data was much lower (4.5 ppm/K) than comparable composition glass (~7 ppm/K). This behaviour was rationalised by assuming that the "effective" T_s of the porcelain in a bilayer, especially at the porcelain–zirconia interface, is greatly reduced because of the thermal gradients present during initial rapid cooling. The subsequent slow re-cooling of the bilayer enabled some additional leucite formation and contributed to a higher porcelain CTE below T_g.

Further detailed modelling of fast cooling of bilayers involving thermo-elastic, structural relaxation and visco-elastic responses associated with the substantial temperature gradients is required.

Acknowledgements

The director of NIOM is thanked for the opportunity for MVS to visit and discuss the results with JT. Dr Enno Bojemueller is thanked for generating the XRD results. Partial support was provided by Kuwait University from Grants (DB01/15) and (SRUL01/14).

REFERENCES

[1] Kelly R, Denry I. Stabilized zirconia as a structural ceramic: an overview. Dent Mater 2008;24:289–98.
[2] Pospiech P, Rountree P, Nothdurft F. Clinical evaluation of zirconia-based all-ceramic posterior bridges: two-year results. J Dent Res 2003;82:114.
[3] Ortorp A, Kihl M, Carlsson G. A 3-year retrospective and clinical follow-up study of zirconia single crowns performed in a private practice. J Dent 2009;37:731–6.
[4] Zembic A, Sailer I, Jung R, Haemmerle C. Randomized controlled clinical trial of customized zirconia and titanium implant abutments for single-tooth implants in canine and posterior regions: 3-year results. Clin Oral Implants Res 2009;20:802–8.
[5] Molin MK, Karlsson SL. Five-year clinical prospective evaluation of zirconia-based Denzir 3-unit FPDs. Int J Prosthodont 2008;21:223–7.
[6] Larsson C, Vult von Steyern P, Sunzel B, Nilner K. All-ceramic two- to five-unit implant-supported reconstructions. A randomized, prospective clinical trial. Swed Dent J 2006;30:45–53.
[7] Al-Amleh B, Lyons K, Swain M. Clinical trials in zirconia: a systematic review. J Oral Rehabil 2010;37:641–52.
[8] Swain MV. Unstable cracking (chipping) of veneering porcelain on all-ceramic dental crowns and fixed partial dentures. Acta Biomater 2009;5:1668–77.
[9] Tholey MJ, Swain MV, Thiel N. Thermal gradients and residual stresses in veneered Y-TZP frameworks. Dent Mater 2011;27:1102–10.
[10] Choi JE, Waddell JN, Swain MV. Pressed ceramics onto zirconia Part 2: indentation fracture and influence of cooling rate on residual stresses. Dent Mater 2011;27:1111–8.
[11] Mainjot AK, Schajer GS, Vanheusden AJ, Sadoun MJ. Influence of veneer thickness on residual stress profile in veneering ceramic: measurement by hole-drilling. Dent Mater 2012;28(2):160–7.
[12] Mainjot AK, Schajer GS, Vanheusden AJ, Sadoun MJ. Influence of cooling rate on residual stress profile in

veneering ceramic: measurement by hole drilling. Dent Mater 2011;27(9):906–14.
[13] Almeida-Júnior AA, Longhini D, Domingues NB, Santos C, Adabo GL. Effects of extreme cooling methods on mechanical properties and shear bond strength of bilayered porcelain/3Y-TZP specimens. J Dent 2013;41(4):356–62.
[14] Isgro G, Kleverlaan CJ, Feilzer AJ. The effects of thermal expansion mismatch and fabrication procedures on the deflection of layered all-ceramic discs. Dent Mater 2005;21:557–61.
[15] Isgro G, Wang H, Kleverlaan CJ, Feilzer AJ. The effects of thermal mismatch and fabrication procedures on the deflection of layered all-ceramic discs. Dent Mater 2005;21:649–55.
[16] Jakubowicz-Kohen BD, Sadoun M, Douillard T, Mainjot AK. Influence of firing time and framework thickness on veneered Y-TZP discs curvature. Dent Mater 2014;30:242–8.
[17] Zhang Y, Lee JJ, Srikanth R, Lawn BR. Edge chipping and flexural resistance of monolithic ceramics. Dent Mater 2013;29(12):1201–8.
[18] Baldassarri M, Stappert CF, Wolff MS, Thompson VP, Zhang Y. Residual stresses in porcelain-veneered zirconia prostheses. Dent Mater 2012;28(8):873–9.
[19] Belli R, Monteiro S, Baratieri LN, Katte H, Petschelt A, Lohbauer U. A photoelastic assessment of residual stresses in zirconia-veneer crowns. J of Dent Res 2012;91(3):316–20.
[20] Ereifej N, Rodrigues FP, Silikas N, Watts DC. Experimental and FE shear-bonding strength at core/veneer interfaces in bilayered ceramics. Dent Mater 2011;27(6):590–7.
[21] Meira JB, Reis BR, Tanaka CB, Ballester RY, Cesar PF, Versluis A, et al. Residual stresses in Y-TZP crowns due to changes in the thermal contraction coefficient of veneers. Dent Mater 2013;29(5):594–601.
[22] Bonfante EA, Rafferty BT, Silva NR, Hanan JC, Rekow ED, Thompson VP, et al. Residual thermal stress simulation in three-dimensional molar crown systems: a finite element analysis. J Prosthodont 2012;21(7):529–34.
[23] Anami LC, Lima JM, Corazza PH, Yamamoto ET, Bottino MA, Borges AL. Finite element analysis of the influence of geometry and design of zirconia crowns on stress distribution. J Prosthodont 2015;24(2):146–51.
[24] Kirsten A, Parkot D, Raith S, Fischer H. A cusp supporting framework design can decrease critical stresses in veneered molar crowns. Dent Mater 2014;30(3):321–6.
[25] Kingery WD, Bowen HK, Uhlmann DR. Introduction to ceramics. 2nd ed. Wiley-Interscience; 1976.
[26] Mackert JR, Evans AL. Quantitative X-ray diffraction of leucite thermal instability in dental porcelain. J Am Ceram Soc 1991;74:450–3.
[27] Mackert JR, Evans AL. Effect of cooling rate on leucite volume fraction in dental porcelains. J Dent Res 1991;70:137–9.
[28] Mackert JR, Khajotia SS, Russell CM, Williams AL. Potential interference of leucite crystallization during porcelain thermal expansion measurement. Dent Mater 1996;12(1):8.
[29] Timoshenko S. Analysis of bi-metal thermostats. J Opt Soc Am 1925;11:233.
[30] Lenz J, Thies M, Schweizerhof K, Rong Q. Thermal stresses in ceramo-metallic crowns: firing in layers. Chin J Dent Res 2002;5(3):5–24.
[31] Kvam K, Hero H. Stress relaxation in titanium-ceramic beams during veneering. Biomaterials 2001;22:1379–84.
[32] Twiggs SW, Mackert JR, Oxford AL, Ergle JW, Lockwood PE. Isothermal phase transformations of a dental porcelain. Dent Mater 2005;21:580–5.
[33] Asaoka K, Kuwayama N. Temperature dependence of the coefficient of thermal expansion and viscosity of dental porcelains. J Jpn Soc Dent Mater Devices 1992;11:250–5.
[34] Asaoka K, Tesk JA. Visco-elastic deformation of dental porcelain and porcelain-metal compatibility. Dent Mater 1991;7:30–5.
[35] Asaoka K. Transient and residual stress in porcelain alloy strip for dental use as affected by tempering. Jpn Soc Mech Eng (JSME) 1991;34:156–62.
[36] Scherer GW. Relaxation in glass and composites. Malabar Florida: Kreiger; 2016. p. 1992.
[37] Tool AQ. Relation between inelastic deformation and thermal expansion of glass in its annealing range. J Am Ceram Soc 1946;29(9):240–53.
[38] Narayanaswamy OS. A model of structural relaxation in gIass. J Am Ceram Soc 1971;54:491–8.
[39] Narayanaswamy OS. Stress and structural relaxation in tempering glass. J Am Ceram Soc 1978;61:146–52.
[40] Ong JL, Farley DW, Norling BK. Quantification of leucite concentration using X-ray diffraction. Dent Mater 2000;16:20–5.
[41] Green DJ, Hannink RHJ, Swain MV. Transformation toughening of Ceramics. Chem Rubber Co.; 2016.
[42] Ritland HN. Density phenomena in the transformation range of a borosilicate crown glass. J Am Ceram Soc 1954;37:370.
[43] Gardon R, Narayanaswamy OS. Stress and volume relaxation in the annealing of flat glass. J Am Ceram Soc 1970;53:380–5.
[44] Hearn EJ. Mechanics of materials, vol. 1, 3rd ed. Butterworth-Heinemann; 2000. p. 62 [chapter 4].
[45] Palmer DC, Dove MT, Ibberson RM, Powell BM. Structural behavior, crystal chemistry, and phase transitions in substituted leucite: high-resolution neutron powder diffraction studies. Am Mineral 1997;82:16–29.
[46] Newton H, Hayward SA, Redfern SAT. Order parameter coupling in leucite: a calorimetric study. Phys Chem Miner 2008;35:11–6.
[47] Taylor D, Henderson CMB. The thermal expansion of the leucite group of minerals. Am Mineral 1968;53:1476–89.
[48] Kvam K, Tibballs JE, Kosmač T. Bond strength and thermal relaxation of 3Y-TZP and dental porcelains. Dublin: Poster, Academy of Dental Materials; 2003.